

# DESIGN AND APPLICATION OF A COLLOCATED CAPACITANCE SENSOR FOR MAGNETIC BEARING SPINDLE

Dongwon Shin, Seon-Jung Liu, Jongwon Kim

Seoul National University  
Seoul, Korea

## SUMMARY

This paper presents a collocated capacitance sensor for magnetic bearings. The main feature of the sensor is that it is made of a specific compact printed circuit board (PCB). The signal processing unit has been also developed. The results of the experimental performance evaluation on the sensitivity, resolution and frequency response of the sensor are presented. Finally, an application example of the sensor to the active control of a magnetic bearing is described.

## INTRODUCTION

A magnetic bearing is a contact-free machine element which can support a spinning shaft by active control of electromagnetic forces. The advantages of magnetic bearings are that they are free from the problem of lubrication, wear, sealing, etc. and that it can actively suppress shaft vibration. However, since the magnetic bearing system is inherently unstable, a feedback controller is necessary. To implement a feedback controller, a displacement sensor is used for on-line measurement of the gap between the rotor and the magnetic bearing pole.

The problem this paper deals with is the location of the sensor. The sensors which are most frequently used are eddy current displacement sensors. This type of sensor is, however, so easily influenced by the magnetic fields generated by the magnetic actuator coils that it should be installed outside the coils (ref. 1). This causes a noncollocation problem of the sensor. The capacitance type sensor is also applied to magnetic bearings (ref. 2). However, commercial capacitance sensors are relatively expensive and are not so compact as to be collocated in the magnetic actuator coils of the magnetic bearing system.

Since the noncollocation problem of the gap sensor means inconsistency of the location of gap measurement with that of magnetic actuator coils, it is natural that the measured gap data include an indispensable error which is proportional to the offset distance of the gap sensor from the center of magnetic actuator coil. Moreover, Maslen *et al.* (ref. 3) and Barrett *et al.* (ref. 4) have verified that the noncollocated magnetic bearing might generate unstable motions with a flexible rotor shaft.

The objective of the research is to develop a collocated sensor system for magnetic bearings. The

main ideas are based on two points. One point is that the developed sensor is of the capacitance types rather than an eddy current type, considering the robustness to electrical noise induced by magnetic fields. The other point is that it is made of a small piece of printed circuit board (PCB) so that it could be both cost-effective and compact enough to be built into the center of the magnetic actuator coils of the magnetic bearing.

The mechanism of gap measurement by using a capacitance type sensor has been well demonstrated by Chapman (ref. 5). Chapman designed a circular sensor plate on which a thin brass layer is coated. He installed this sensor plate at the end of the spindle nose of a milling machine in such a way that the sensor plate and the spindle nose maintain a sub-mm gap from each other. He used this sensor system in on-line measurement of the gap, thus ultimately measuring the rotational motion accuracy of the spindle axis.

The research approach used in this paper is based on Chapman's method. What has been enhanced is that the sensor size can be reduced by the order of more than 1:200 by adopting PCB manufacturing technology instead of a man-made brass layer. Additionally, the signal processing unit is refined for improving the resolution and bandwidth of the sensor system, which becomes more critical as the sensor size gets smaller.

This paper is organized as follows. In the next section, the detailed design of the collocated capacitance sensor system is described. Then, the following section presents the experimental setup and the results of the experimental evaluation of the developed sensor system. Finally, the experimental results of the sensor system application to magnetic bearing control are included.

## DESIGN OF A COLLOCATED CAPACITANCE SENSOR SYSTEM

The overall shape and location of the gap sensor plate is illustrated below in figure 1. The base material of the sensor plate is epoxy resin FR4 with a copper layer coated on it. The coating thickness is 0.1 mm.

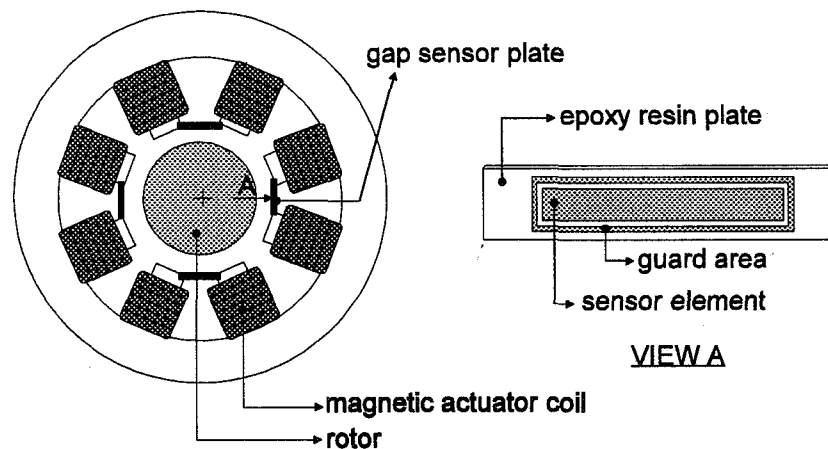


Figure 1. Cross section of the magnetic bearing and the overall shape and location of the gap sensor plate.

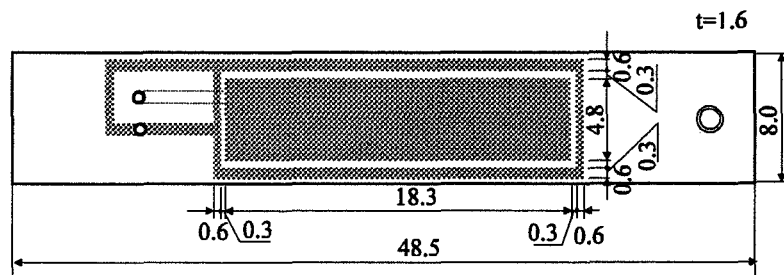


Figure 2. Detail geometric dimensions in mm of the gap sensor plate.

The copper layer is then cut out to the desired pattern through the etching process, which is an identical technology to the manufacture of printed circuit boards (PCB's). The copper layer pattern is composed of a sensor element and a guard area. The guard area, surrounding the sensor element, protects the sensor element from the influence of the electromagnetic fields outside the sensor plate. As shown in figure 1, a sensor plate is embedded into each of the magnetic actuator coils in order. The location of the sensor plate in the center position of the magnetic actuator coil eliminates definitely the noncollocation problem of the sensor.

Figure 2 shows the detailed geometric dimensions of the gap sensor plate developed. Currently, sensor plate of width 8.0 mm, length 48.5 mm and thickness 1.6 mm are manufactured. The capacitance of the sensor is 1.95 pF when the gap between the rotor and the sensor is 0.4 mm. Finally, the surface of the sensor plate is coated with an insulator.

Two pairs of gap sensors are connected to one signal processing unit as shown in the schematic diagram of figure 3. Each of x and y axis gap displacements is measured by each pair of gap sensors located opposite to each other. The signal processing unit consists of two parts : (1) four channels of capacitance to voltage converters (C/V's), sample and holders (S/H's), low pass filters (LPF's), offset and gain adjustment circuits (OGA's), and (2) two channels of differential circuits (DIFF's), offset and gain adjustment circuits (OGA's).

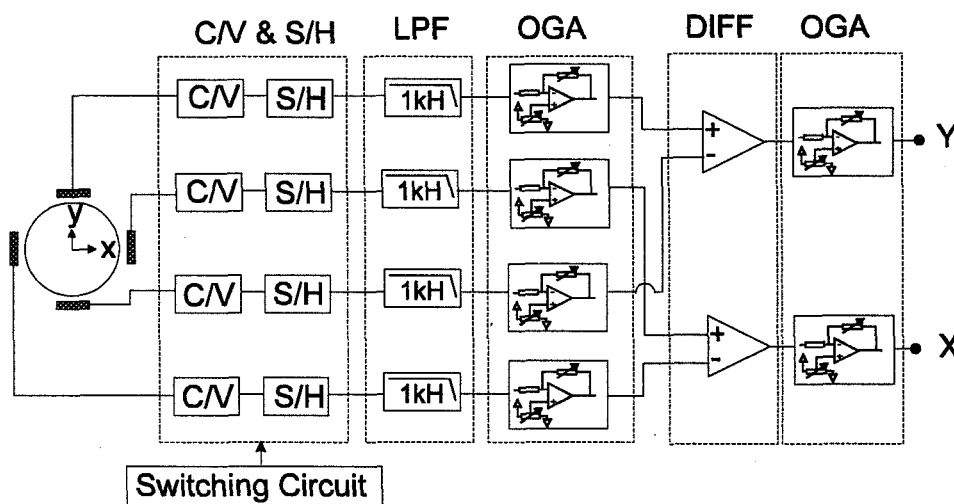
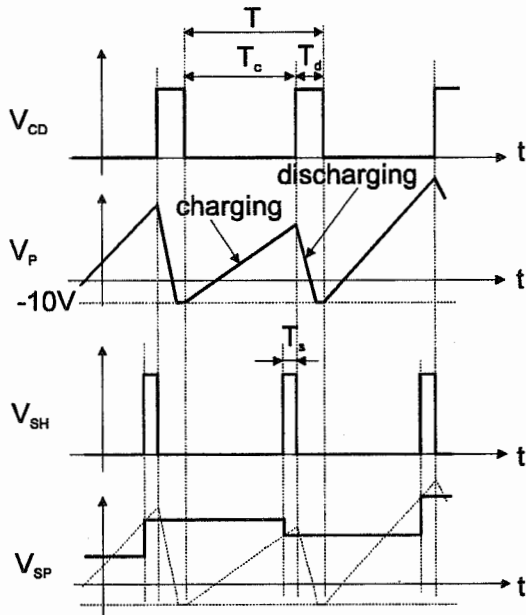
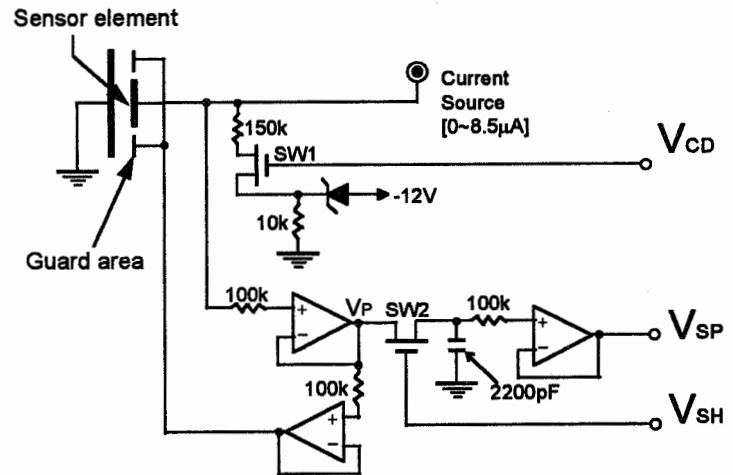


Figure 3. Schematic diagram of the signal processing unit.

The C/V converter charges the sensor element of the sensor plate during a fixed charging time interval  $T_c$ , and then measures and holds the charged voltage  $V_P$  of the sensor element. After sampling and holding  $V_P$  it discharges remaining electric charges on the sensor element during a fixed discharging time interval  $T_d$ . The C/V converter repeats this charging, sampling and holding, and discharging routine during a total time interval  $T$ . Figure 4-a. shows the signal flow chart of the C/V converter.



(a) Signal flow chart



(b) Detail circuits of C/V and S/H

Figure 4. Signal flow chart and detail circuits of the C/V and S/H of the signal processing unit.

The gap between the rotor and the magnetic actuator coil, denoted by  $x$ , is related to the fixed charging time interval  $T_c$  and the charged voltage  $V_P$  of the sensor element as following :

$$V_P = \frac{Q_{T_c}}{C_s} \equiv \frac{\int_0^{T_c} i_s dt}{\kappa \epsilon_0 A_s} x \quad \text{or} \quad V_P = \frac{i_s T_c x}{\kappa \epsilon_0 A_s} \quad (1)$$

where

$Q_{T_c}$ : electric charges accumulated during  $T_c$

$C_s$ : capacitance of the sensor element

$i_s$ : current input to the sensor element

$\kappa$ : dielectric constant

$\epsilon_0$ : permittivity constant

$A_s$ : total area of the sensor element

From equation (1), the displacement gap  $x$  is measured indirectly from the charged voltage  $V_P$ . Figure 4-b illustrates the detailed circuits of the C/V and S/H of the signal processing unit. In order to charge the sensor element, Chapman (ref. 6) used a constant voltage source. With a constant voltage source, the rate of growth of the charged voltage  $V_P$  decreases during the charging time interval  $T_c$ ,

resulting in the deterioration of measurement resolution as the gap  $x$  becomes larger. For this reason, a constant current source circuit is adopted in order to maintain a linear increase of  $V_p$  during  $T_c$ . The driving signal  $V_{CD}$  synchronizes the charging and discharging cycle of the sensor element by turning on and off switch #1 (SW1) in the circuit as shown in figure 4. On the other hand, the sample and hold driving signal  $V_{SH}$  turns on and off switch #2 (SW2) in the circuit. Therefore the maximum value of the charged voltage  $V_p$  of the sensor element is sampled and held, thus being transformed to the output signal  $V_{SP}$  of the C/V and S/H circuit. The typical values of cycle time  $T$ , discharging time  $T_d$ , sample and holding time  $T_s$  are 50-100  $\mu\text{sec}$ , 15  $\mu\text{sec}$ , and 440 nsec, respectively.

The low pass filter (LPF) of the signal processing unit (see figure 3) eliminates the switching noise component of the output signal  $V_{SP}$  with the cutoff frequency of 1 kHz. The function of the offset and gain adjustment circuit (OGA) is to compensate for the inherent tolerance of the geometric dimension of the sensor element and for the electric properties of each channel in the signal processing unit.

As shown in figure 3, a pair of gap sensors is assigned to each axis gap measurement. Each pair of sensors is located in the opposite direction from each other. What is necessary to obtain from this sensor system for magnetic bearing control is the relative displacement of the rotor from the fixed reference of frame. That is, the difference between the output signals from the sensor elements of the same pair is important for magnetic bearing control. Hence, the output signals from the sensor elements constituting a pair are finally differentiated, and then, amplified by the differential circuits (DIFF's) of the signal processing unit, resulting in  $V_x$  and  $V_y$ .

## EXPERIMENTAL EVALUATION OF THE DEVELOPED SENSOR SYSTEM

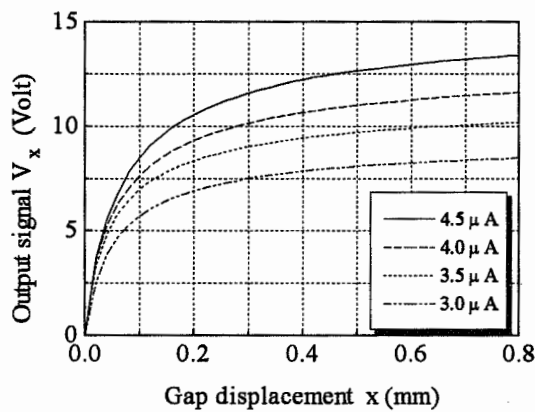
As the performance measures of the developed sensor system, the sensor sensitivity and bandwidth subject to static and dynamic gap displacement variations, respectively, are evaluated.

### Sensor Sensitivity to the Static Gap Displacement Variation

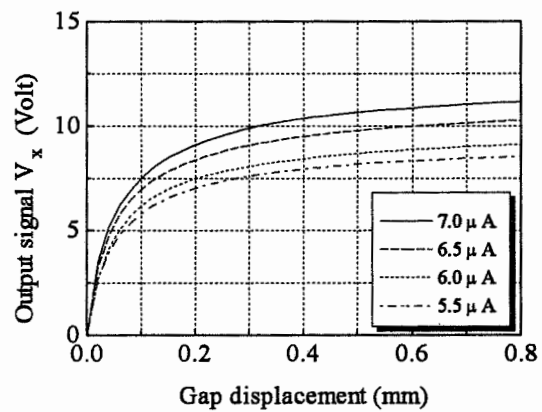
An experimental setup has been implemented such that a sensor plate is attached to the moving part of a micrometer which retains the positioning accuracy of 0.01 mm resolution. The sensor plate is able to be positioned accurately from the rotor shaft in radial direction by using the micrometer. For each positioning point of the sensor plate, that is, for each known gap displacement, the output signals of the signal processing unit are measured. The experimental results are shown in figure 5.

The sensitivity plots shown in figure 5 are obtained from two series of experiments in cases of the cycle time  $T$  of 97  $\mu\text{sec}$  and 65  $\mu\text{sec}$ , respectively. The discharging time  $T_d$  is 15  $\mu\text{sec}$  for both cases. The constant current  $i_s$  supplied to the sensor element is also varied from 3.0  $\mu\text{A}$  to 7.0  $\mu\text{A}$ . From the plots, sensitivity characteristics can be easily verified as follows :

- (1) As the cycle time  $T$  increases, the range of the sensor increases,
- (2) as the output of the current source  $i_s$  increases, the range of the sensor increases, and
- (3) the rate of growth of the output signal  $V_x$  decreases as the gap displacement  $x$  increases.



(a) In case of  $T=97\mu\text{sec}$



(b) In case of  $T=65\mu\text{sec}$

Figure 5. Sensor sensitivity to the static gap displacement variation.

Since the relationship between the output signal  $V_x$  and the gap displacement  $x$  is not linear, a look-up table method or an interpolation algorithm should be used when utilizing indirect measurement data to practical control issues.

#### Bandwidth to the Dynamic Gap Displacement Variation

The bandwidth of the sensor is also important when it is used for magnetic bearing control at such high rotational speeds above 10,000 rpm. To test the bandwidth of the sensor, the gap displacement  $x$  has to be varied in such a way to generate a sinusoidal signal. For this purpose, a special rotor shaft has been designed and manufactured. The cross section of the specially designed rotor shaft is shown in figure 6.

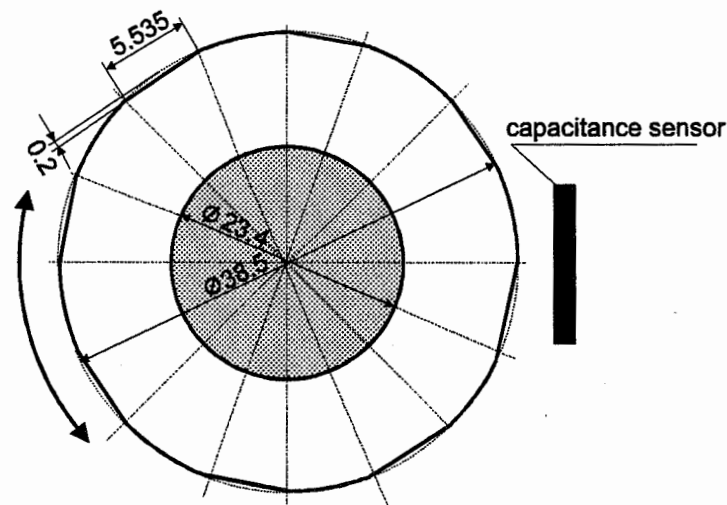


Figure 6. Cross section of the specially designed rotor shaft for the sensor bandwidth test[unit : mm]

Eight segments of the perimeter of the rotor shaft with the diameter of 38.5 mm have been flat end-milled at equiangular intervals with the width and the maximum depth-of-cut of 5.535 mm and 0.2 mm, respectively. Thus, the specially designed rotor shaft is able to generate quasi-sinusoidal gap displacement signals of the maximum frequency of 1.6 kHz when its spinning speed is 12,000 rpm.

The frequency response plots of the output signal  $V_x$  are shown in figure 7. The Bode plots shown in figure 7 are obtained from the three series of experiments in cases of the cycle time  $T$  of 97, 65 and 57  $\mu\text{sec}$ , respectively. The discharging time  $T_d$  is 15  $\mu\text{sec}$ , and the constant current  $i_s$  is 4.5, 7.0 and 7.5  $\mu\text{A}$ , respectively. From the plots, frequency response characteristics can be easily verified as follows :

- (1) As the cycle time  $T$  decreases, the bandwidth of the sensor increases, and
- (2) the bandwidth of the sensor with  $T$  of 97  $\mu\text{sec}$  is around 7,500 rad/sec (or 1.2 kHz).

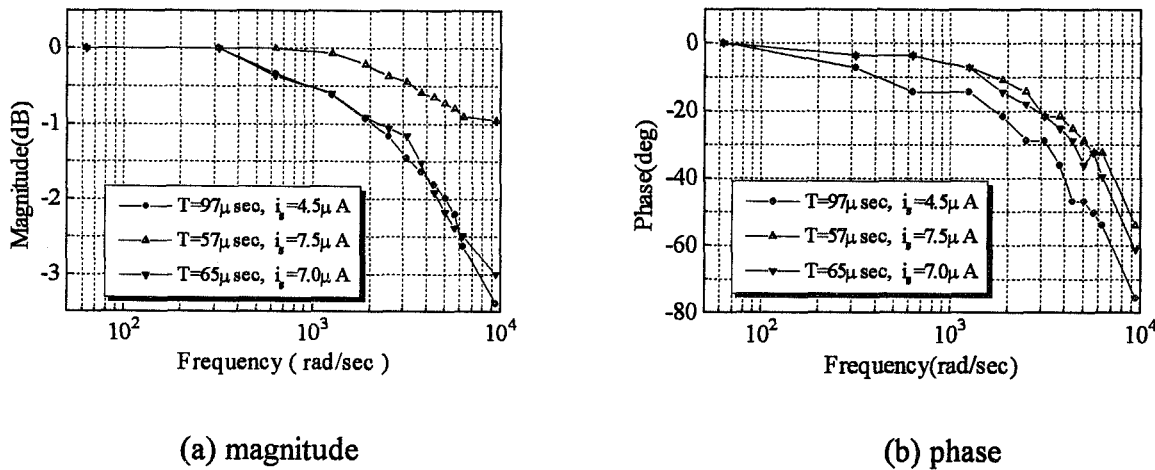


Figure 7. Frequency response of the output signal  $V_x$

If higher bandwidth is desired, a lower value of the cycle time  $T$  should be selected. In this case, the static sensitivity is decreased as shown in figure 5. From further experimental results, of which data are not shown in the paper, it has been also verified that the bandwidth of the sensor is independent of both the output of the current source  $i_s$  and the total area of the sensor element  $A_s$ .

### SENSOR APPLICATION TO A MAGNETIC BEARING SPINDLE

The collocated sensor system has been equipped into a testbed of a magnetic bearing spindle as shown in figure 8 on the next page. The vertical rotor shaft is supported by a radial angular contact ball bearing at the lower part and by a radial magnetic bearing at the upper part. Thus, without the magnetic bearing, the rotor shaft would behave like a vertical pendulum. The rotor is connected to a brushless DC motor through a universal coupling. From the built-in encoder in the DC motor, the spinning speed of the rotor shaft is measured. There is a backup ball bearing at the uppermost part of the rotor for both idle and emergency states.

The feedback control algorithm is run by a digital signal processor (DSP) based controller where a TMS320C40 CPU chip is embedded with a 12-bit analog-to-digital (A/D) converter and a 12-bit digital-to-analog (D/A) converter. The DSP board is installed into a personal computer 486 class. PC 486 can share the selected internal states with the DSP board through a dual port random access memory (RAM) of the DSP board. Based upon the output of the DSP board, a pulse width modulation (PWM) current amplifier generates each of the control inputs into two pairs of magnetic actuator coils which drive independently the x and y-axis radial motions of the rotor shaft, respectively.

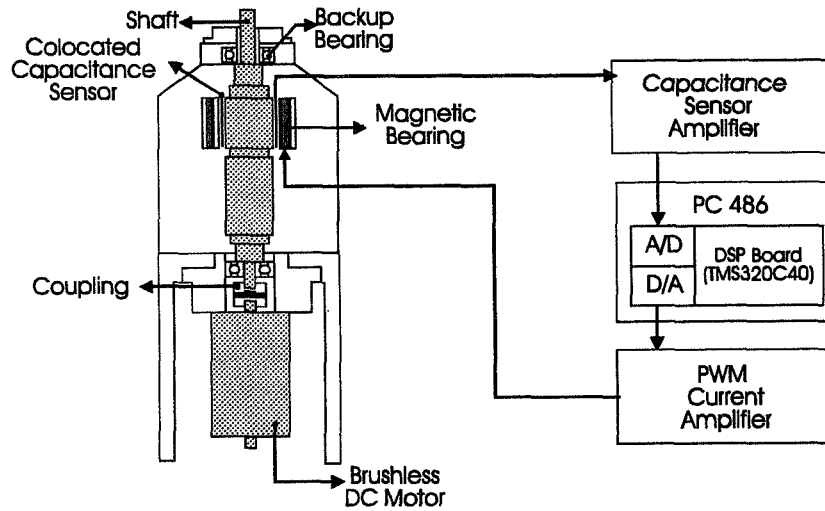


Figure 8. Schematics of a testbed for the magnetic bearing control experiment by using the collocated gap displacement sensor.

The feedback control algorithm adopted for magnetic bearing control is one of modified PID controllers, which might be called an 'I-Lead' feedback controller :

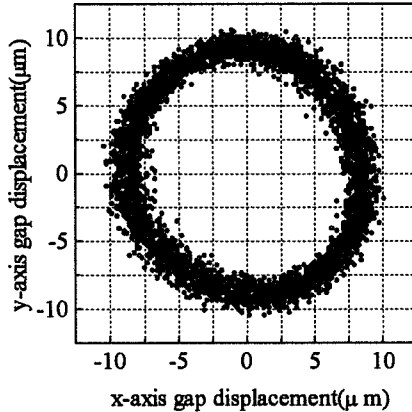
$$\frac{I_j(s)}{V_j(s)} = K_c \frac{s+b}{s+a} + \frac{K_I}{s}; \quad j = x, y \quad (2)$$

where  $I_j(s)$  : Laplace transform of the variation of control inputs to magnetic actuator coils  
 $V_j(s)$  : Laplace transform of the variation of gap displacement signals  
 $K_c, K_I$  : Controller gains

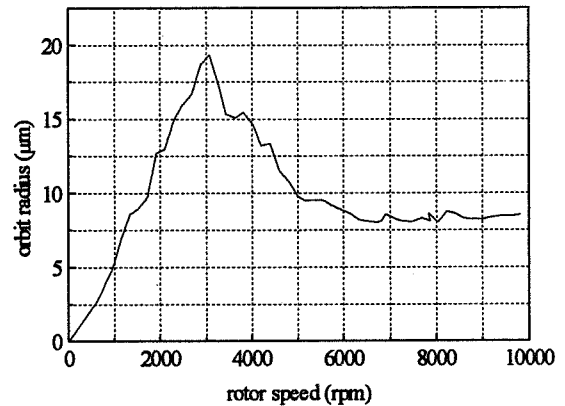
In the experiment, the controller parameters are selected as  $K_c = 21,000$  A/m,  $a = 9,545$  rad/sec,  $b = 1,363$  rad/sec,  $K_I = 1,500$  A/m-sec, and the control sampling time  $T_{cn} = 0.1$  msec. Among the output signals from the sensor signal processing unit, the maximum bound of the noise signal has been measured to be around 30 mV, which corresponds to the gap displacement of  $2.3\mu\text{m}$ . This value is the final resolution of the collocated sensor system.

Figure 9 on the next page shows the experimental results of the magnetic bearing control where the developed collocated sensor system has been utilized. Figure 9-a presents the orbit of the rotor





(a) Rotor orbit at 5,800rpm



(b) Orbit radius with varying rotor speed

Figure 9. Experimental results of the magnetic bearing control by using the collocated gap displacement sensor.

shaft center when it is spinning at 5,800 rpm. The average orbit radius is around 9  $\mu\text{m}$ . The average orbit radii have been recorded as the rotational speed is varied up to 10,000 rpm as shown in figure 9-b. At the natural frequency of 320 rad/sec (that is, at the spinning speed of 3,060 rpm), the average orbit radius reaches the maximum value of 19  $\mu\text{m}$ .

## CONCLUSIONS

(1) A collocated sensor system has been developed for magnetic bearing control application. It consists of a capacitance type gap sensor plate constructed by applying PCB manufacturing technology and a signal processing unit for measuring and amplifying the charged voltages of the sensor element of the sensor plate during a cycle time of less than 100  $\mu\text{sec}$ .

(2) The sensor sensitivity and bandwidth subject to static and dynamic gap displacement variations, respectively, are measured in the experiments. The bandwidth of the sensor is measured to be 1.2 kHz when the cycle time is 97  $\mu\text{sec}$ .

(3) The experimental works have been executed to verify the function of the collocated sensor system. The sensor has been embedded into a vertical magnetic bearing spindle system. The average orbit radii of the rotor shaft center have been obtained increasing the rotor rotational speed up to 10,000 rpm, with the maximum value of 19  $\mu\text{m}$  at the speed of 3,060 rpm.

## REFERENCES

1. Allaire, P. E.; and Humphris, R. R.: Dynamics of a Flexible Rotor in Magnetic Bearings. *4th Workshop on Rotor Dynamics Instability Problems in High Speed Turbomachinery*, Texas A&M Univ., June 1986.
2. Ortiz Salazar, A., Dunford, W., Stephan, R.; and Watanabe, E.: A Magnetic Bearing Systems Using Capacitive Sensor for Position Measurement. *IEEE Trans. on Magnetics*, Vol. 26, No. 5, Sept. 1990, pp2541-2543.
3. Maslen, E. H.; and Lefante, V. S.: Transfer Function Zeros in Noncollocated Flexible Rotor Models. *Proceedings of the 3rd International Symposium on Magnetic Bearings*, 1992, pp242-252.
4. Barrett, L. E.; Brockett, T. S.; and Maslen, E. H.: Analysis of Rotors with Non-Collocated Magnetic Bearings Using Transfer Matrices. *Proceedings of MAG '92*, 1992, pp144-154.
5. Chapman, P. D.: A Capacitive Based Ultra-precision Spindle Error Analyzer. *J. of Precision Engineering*, Vol. 7 No. 3, July 1985, pp29-536.